Mechanical properties and self-sensing ability of graphene-mortar compositions with different water content for 3D printing applications

Materials Today: Proceedings 70 (2022) 412–417

Contents lists available at ScienceDirect

Materials Today: Proceedings

journal homepage: www.elsevier.com/locate/matpr

Mechanical properties and self-sensing ability of graphene-mortar compositions with different water content for 3D printing applications

A Dulaj *, T.A.M. Salet, S.S. Lucas

Eindhoven University of Technology, Eindhoven, the Netherlands

ARTICLE INFO

Article history:
Available online 24 September 2022

Keywords:
3D printed concrete
Self-sensing
Graphene nanoplatelets
Hardened state properties

ABSTRACT

There is an increasing ongoing research on concrete compositions with enhanced properties such as self sensing given by the use of carbon nanomaterials. Carbon nanotubes-cement composites have been studied for over a decade to produce smart materials, with interesting results. However, since first synthetized in 2004, Graphene is rapidly growing in popularity due to similar conductive properties, high stiffness and strength, lower environmental impact and ease of production and lower production prices. More recent studies have tried to incorporate this material into concrete compositions with positive results. On the other hand, the construction industry is moving towards more automated production processes and new technologies such as 3D printing concrete are gaining popularity. However, there is little research on the effects of nanomaterials in 3D printable concrete compositions.

In this paper, the effects of Graphene nanoplatelets (GnPs) on a the mechanical properties and conductivity of a printable mortar are investigated. Five different compositions with different water content and graphene content were prepared to create cast and printed samples with dimensions 40x40x160 mm^3 that were tested to evaluate the mechanical strength and the resistivity change between unloaded and loaded to failure conditions. A linear regression model using Matlab was created to have an overview on the strength and resistivity change depending on the water-cement ratio (w/c) and Graphene nanoplatelet content (GnP).

The results showed that in cast samples, GnPs improve the compressive strength and the self sensing ability of the material, while in printed samples, GnPs has a detrimental effect on the compressive strength and the self sensing ability depends heavily on the printed layers direction. Future studies should concentrate on the effect of interlayer adhesion on the self sensing and mechanical properties, and on the additives necessary to improve the printability of GnP-mortar compositions.

1. Introduction

Graphene is a new material that was first isolated and investigated in 2004 [1,2]. It is a two-dimensional nanomaterial, composed of carbon atoms arranged in a honeycomb structure to create nanoplatelets with a large specific surface area, high Young's modulus, high stiffness values and fracture strength [3]. There is a growing interest in graphene nano-platelets (GnPs) in the construction industry since its numerous properties (mechanical, thermal, electrical) enhance the properties of concrete when mixed together in very small quantities by improving its strength and providing smart functionalities such as self-sensing [4]. Furthermore, the increase in graphene production is leading to a reduction in costs and its environmental impact, proving to be less harmful than Portland cement (CEM I) [5]. Therefore, graphene-concrete composites are being studied for both reinforcement applications and self-sensing applications in order to create a material with an embedded health monitoring system and increased durability [6].

At the same time, the construction industry is moving towards more automated manufacturing processes which can bring advantages over traditional concrete. 3D concrete printing (3DCP) is being studied as a possible alternative to traditional construction techniques thanks to the lower use of material and labor, greater freedom in construction shapes and relatively low costs [7,8]. Although research on the mix design of concrete for this new

* Corresponding author.

https://doi.org/10.1016/j.matpr.2022.09.278

technology in underway, the use of nanomaterials such as GnPs with a printable concrete is still a novelty.

In this study, graphene nanoplatelets were mixed with a printable mortar to improve the strength and alter the conductivity of the composition, and their effects were investigated. Parallelly, the effect of different water contents in the mortar was analyzed. Five compositions were prepared with different water content and graphene content; the mixes were cast into standard molds and the mechanical properties and the resistivity at hardened state were measured. A model was then created using linear regression with MATLAB to find the better combination for strength and self-sensing applications. Finally, the composition with better performance was printed and the conductivity and mechanical strength were measured and compared to cast samples.

2. Materials and methods

2.1. Materials and samples preparation

The printable mix composition used in this paper is reported in Table 1.

As reported in Table 1, three different contents of water and graphene were used to prepare 5 mixtures with 5 different combinations reported in Table 2. All the other components were kept unchanged.

The graphene nanoplatelets used in this paper are produced by Nanografi Nanotechnology AS. The graphene was first dispersed in the mortar's water with superplasticizer using an ultrasonic bath for 40 min. The solution was then added to the dry materials which were previously mixed together with a mixer, and mixed for 5 min to prepare the mortar. The fresh mix was then poured into standard foam molds with dimension of 40x40x160 mm^3 and covered in plastic for 24 h to prevent moisture loss. After 24 h the samples were cured in water for 28 days.

The printed samples were prepared and mixed in the same way and the resulting mortars were printed with the same dimensions using an ABB IRB 1200 robot combined with a Makita DCG 140 Caulking gun (Fig. 1). The specimens were covered in plastic for 24 h and cured in water for 28 days.

2.2. Mechanical test

The mechanical tests were performed according to BS EN 1015–11:1999: a 3-point bending test and a compression test were performed after 7 days and 28 days of curing on both cast and printed specimens. Both tests were performed in load control with a load speed of 50 N/s for the bending test, and 2400 N/s for the compression test. The flexural strength was determined by Eq. (1).

Table 1
Composition of the printable mortar.

Composition	Mix ratio	Type
Sand	sand–binder ratio = 1.5	CEN-NORMSAND DIN EN 196–1
Binder	80 % cement 20 % limestone	CEM I 52.5R Heidelberg cement Weber Beamix
Water	Water-binder ratio = 0.25, 0.375, 0.5	
Additives (per binder content)	1.2 % superplasticizer	Sika® ViscoCrete®-2640 con. 35 % SPL
	Graphene content = 0 %, 0.6 %,1.2 %	Nanographi Nanotechnology. Purity: 99.9+%, Size: 5 nm, S.A: 170 m2/g, Dia: 7 μm

$$f_b = 1.5 \cdot F \cdot \frac{l}{b \cdot d^2} \quad (1)$$

The compression strength was determined by Eq. (2).

$$f_c = F/(b \cdot l) \quad (2)$$

Where l = length, b = width and d = height of sample. F is the force that leads to failure.

The printed samples where tested in two different layer directions in bending (Fig. 2) and in compression (Fig. 3).

2.3. Resistivity measurements

The resistivity was measured for both cast and printed samples in both layer directions (see Fig. 4) after 28 days of curing in water. The samples, with dimensions 16x4x4 cm^3, were subjected to compression strain in a displacement controlled setup using an Instron instrument with a head speed of 0.5 mm/min. The resistivity was measured and recorded every 3 s while the compression strains were applied until failure, using Resipod, a surface resistivity meter for concrete from Proceq.

3. Experimental results and discussion

3.1. Cast samples

3.1.1. Mechanical test

The results of the mechanical tests for cast specimens are reported in Table 3 and Fig. 5.

As seen in Table 3 and in Fig. 5, the compression strength increased when 1.2 % of GnP per binder content were added to the mortar. This could be explained by the fact that GnPs help to create a more homogeneous and dense matrix, acting both as a filler and as a nucleation point for cement hydration. The bending strength seemed not affected by the presence of GnP.

An overview of the development of the compressive strength is reported in Fig. 6. The model was calculated using a linear regression in Matlab.

The function plotted in Fig. 6 is described by Eq. (3).

$$C = 111.4 + 27.2G - 148.8W - 12.0G \cdot W - 16.1G^2 \quad (3)$$

With C = compression strength (MPa), G = GnP percentage per binder content (%), W = water cement ratio (w/c) and a R^2 of 0.978.

As seen in Fig. 6, the function has a maximum at w/c = 0.25 and GnP content of 0.8 % per binder content.

3.1.2. Resistivity test

The results of the resistivity measurement tests for cast specimens are reported in Table 4 and Fig. 7.

As seen in Table 4 and Fig. 7, the samples with GnP were more sensitive to strain than samples without GnP and the resistivity change was bigger. The water content had an influence on the results as well: the samples with higher water-cement ratio resulted in a lower resistivity in unloaded conditions due to the higher presence of free water in the matrix. However the resistivity change seems to depend mostly on the presence of GnPs than on the water content.

An overview of the development of the resistivity change is reported in Fig. 8. The model was calculated using a linear regression in Matlab.

The function plotted in Fig. 8 is described by Eq. (4).

$$R = 47.7 - 28.7G - 32.8W - 11.7G \cdot W + 43.8G^2 \quad (4)$$

With R = resistivity change (%), G = GnPs percentage per binder content (%), W = water cement ratio (w/c) and a R^2 of 0.978.

Table 2
Five mixes tested with changing water and graphene content.

	A	B	C	CB	ABC
Graphene (% per binder content)	0 %	1.2 %	0 %	1.2 %	0.6 %
Water/cement ratio	0.25	0.25	0.5	0.5 %	0.375

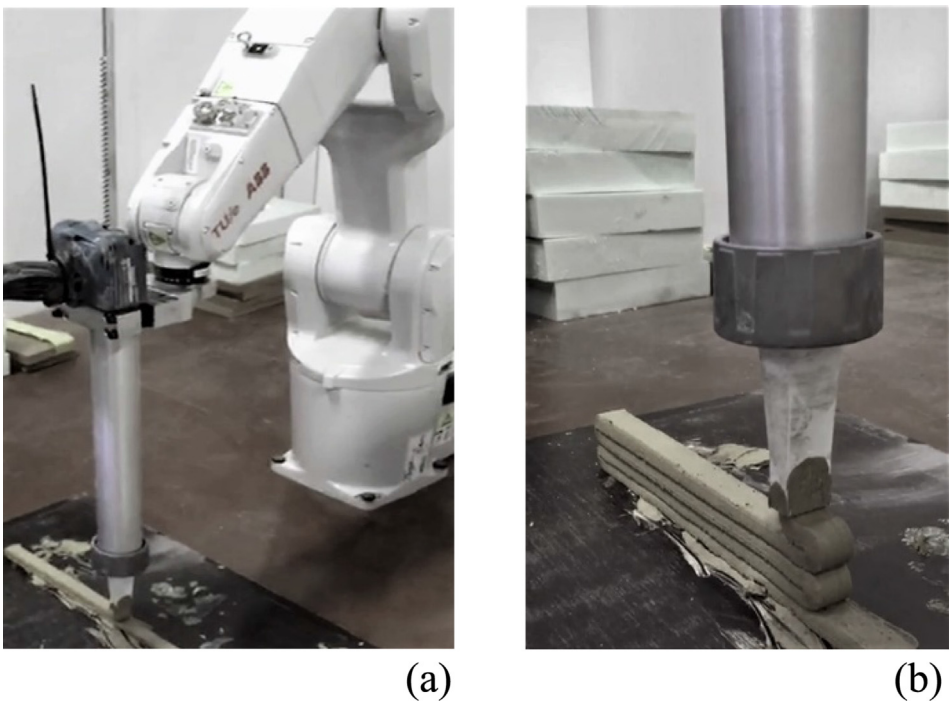

Fig. 1. a) ABB IRB 1200 robot combined with Makita DCG 140 Caulking gun and b) printing of samples.

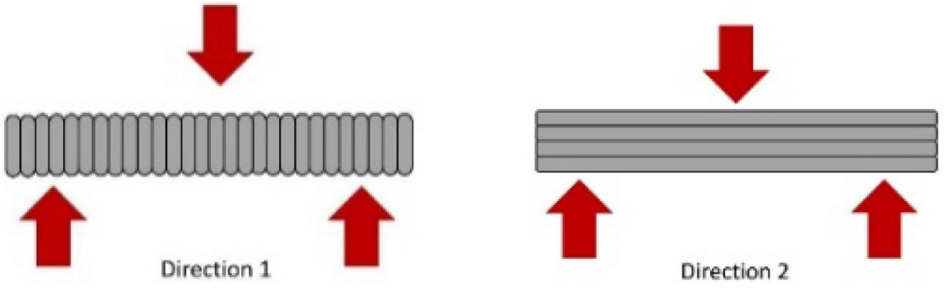

Fig. 2. Printed samples testing direction for the 3-point bending test.

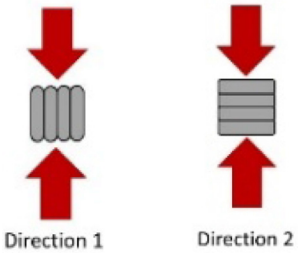

Fig. 3. Printed samples testing direction for the compression test.

As seen in Fig. 8, the function has not a maximum but has the highest value at w/c = 0.25 and GnPs content of 1.2 % per binder content.

3.2. Printed samples

The compositions printed were only the ones with water-cement ratio of 0.25 (A and B) for two main reasons: they were the ones with higher resistivity change, which means more sensitive to stresses and strains changes, and the compositions with water-cement ration of 0.375 and 0.5 were not printable, being too liquid due to the higher water content.

3.2.1. Mechanical tests

The results of the mechanical tests for printed specimens are reported in Table 5 and Fig. 9.

As seen in Table 5 and Fig. 9, both the compression strength and the bending strength of the printed samples with 1.2 % GnP per binder content decreased compared to the cast samples and to the ones without GnPs. This is probably due to the fact that the

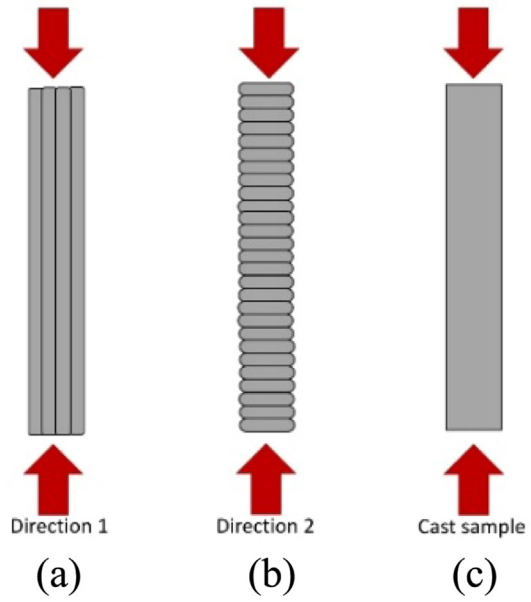

Fig. 4. Samples subjected to compression strains for resistivity measurements a) printed sample with layer direction 1, b) printed sample with layer direction 2 and c) cast sample.

Table 3
Compression and bending strength of cast samples after 7 days of curing.

Sample	Compression strength (MPa)	Bending strength (MPa)
A	74.2	10.9
B	80.0	10.6
C	37.0	4.7
CB	39.2	5.2
ABC	63.4	7.8

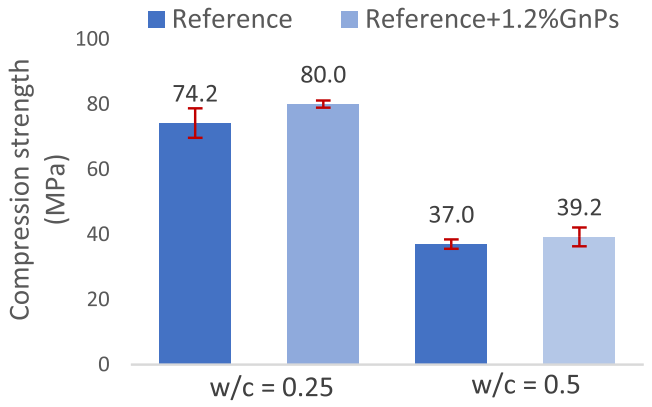

Fig. 5. Compression strength of cast samples with different water content (w/c = 0.25 and w/c = 0.5) and GnP content (GnP content = 0 % and 1.2 % per binder content).

samples without GnPs had better interlayer adhesion since the addition of GnP made the material less flowable. On the other hand, the high flowability of the compositions without GnPs made them more difficult to be printed with the ABB robot. This test was useful to understand how the interlayer adhesion can affect the results and what do the compositions need to improve the printing process. For future research, the addition of other additives such as accelerator, and the change in the superplasticizer content will need to be investigated to improve the printability of the mixes.

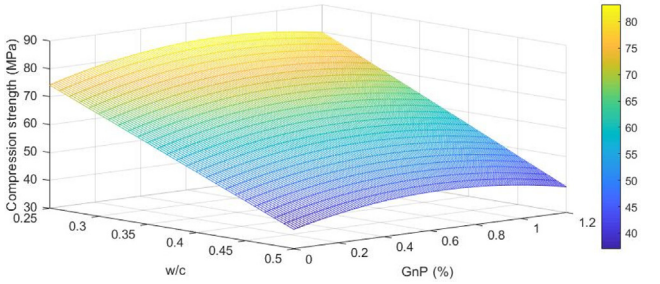

Fig. 6. Compressive strength development of the mixes depending on water and GnP content, calculated with a linear regression model in Matlab.

Table 4
Resistivity of unloaded cast samples and resistivity change up until failure of cast samples after 7 days of curing.

Sample	Resistivity of unloaded samples (kΩcm)	Resistivity at failure (kΩcm)	Resistivity change up until failure (%)
A	23.3	14.1	39.5
B	47.0	16.6	64.7
C	4.8	3.3	31.3
CB	7.3	3.4	53.1
ABC	7.4	5.1	31.2

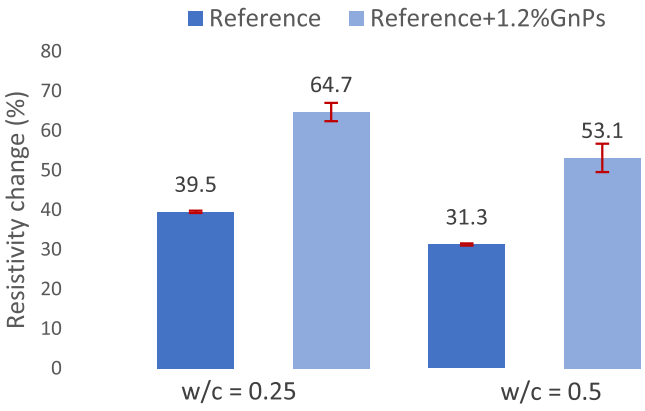

Fig. 7. Resistivity change between unloaded to loaded cast samples up until failure, with different water content (w/c = 0.25 and w/c = 0.5) and GnP content (GnP content = 0 % and 1.2 % per binder content).

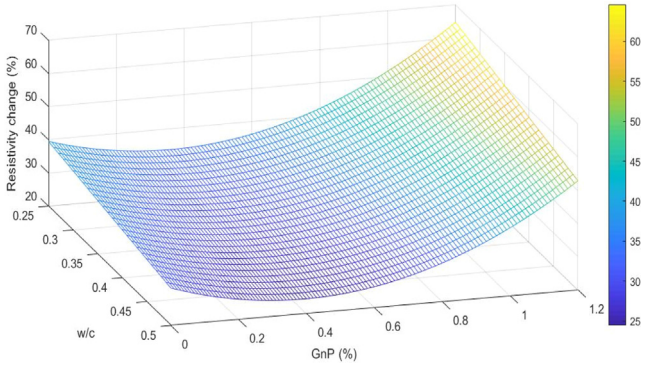

Fig. 8. Matlab model of the resistivity change in a composition subjected to compression, depending on water content and GnP content.

Table 5
Mechanical strength of printed samples with different GnP content (GnP content = 0 % and 1.2 % per binder content) and layer direction (direction 1 and direction 2; see Figs. 2 and 3).

Layers direction	Sample	Compression strength (MPa)	Bending strength (MPa)
Direction 1	A	64.5	12.3
	B	57.9	9.9
Direction 2	A	71.4	14.0
	B	62.0	12.2

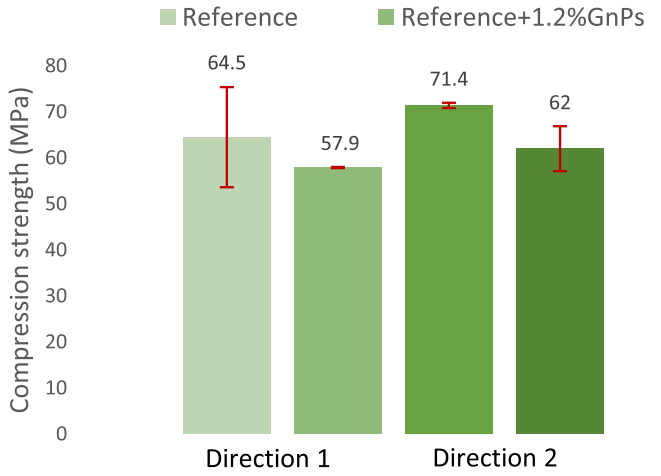

Fig. 9. Compression strength of printed samples with different GnP content and layers direction.

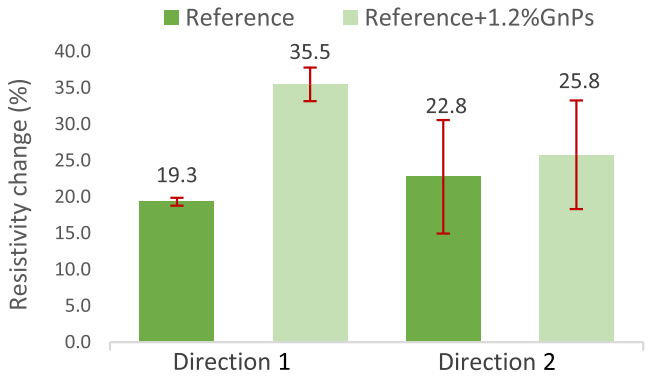

Fig. 10. Resistivity change between unloaded to loaded printed samples up until failure, with different GnPs content and layer directions.

3.2.2. Resistivity test

In Fig. 10 is plotted the resistivity decrease (%) between unloaded and loaded until failure of the printed samples for both layers directions.

As seen in Fig. 10, the samples with GnPs were the ones most affected by the printing process, in accordance with the compression strength results of section 3.2.1. In both layers directions the resistivity change increased with the presence of GnPs. However, for direction 2 the increase was nearly imperceptible compared to the samples without GnPs, and this can be explained again by the lower interlayer adhesion that the GnPs presence could cause.

For future research, the interlayer adhesion and its improvement should be investigated with targeted tests.

4. Conclusion

In this study, the effects of the water content and GnPs content on the mechanical properties and resistivity of concrete mortars were investigated. Cast and printed samples were prepared ad the results of the tests were compared to assess the effects of the printing process, layers directions and interlayer adhesion.

The results show that when compressive strains are applied to the mortars, the resistivity decreases, in accordance to previous research [9–11]. The samples with graphene showed a higher sensitivity to the applied strain (higher change in resistivity) in both cast and printed samples. However, the presence of GnPs in the printed samples with layers direction 2 (see Fig. 3) didn't improve much the self sensing ability of the material (the difference of resistivity change between the reference samples and the samples with GnPs was very small) and this can be explained by a worse interlayer adhesion due to a reduced flowability of the mortar caused by GnPs presence. All the other combinations showed positive results with an increase of sensitivity GnPs were added to the mixes.

The mechanical results showed an improvement in compressive strength up to 20 % for cast samples with GnPs, while the strength decreased for printed samples in both layers directions, which again can be explained by a poorer interlayer adhesion.

For future research, the printable composition should be modified by the using additives to improve the printing quality and targeted tests should be performed to investigate and improve interlayer adhesion.

Data availability

Data will be made available on request.

Declaration of Competing Interest

The authors declare the following financial interests/personal relationships which may be considered as potential competing interests: Albanela Dulaj reports financial support was provided by Dutch Research Council.

References

[1] K.S. Novoselov, A.K. Geim, S.V. Morozov, D. Jiang, Y. Zhang, S.V. Dubonos, I.V. Grigorieva, A.A. Firsov, Electric field effect in atomically thin carbon films, Science 306 (5696) (2004) 666–669, https://doi.org/10.1126/science.1102896.
[2] This Month in Physics History: October 22, 2004: Discovery of Graphene. APS News. Series II. 18 (9): 2. 2009
[3] B. Wang, B. Pang, Mechanical property and toughening mechanism of water reducing agents modified graphene nanoplatelets reinforced cement composites, Constr. Build. Mater. 226 (2019) 699–711, https://doi.org/10.1016/j.conbuildmat.2019.07.229.
[4] E. Shamsaei, F. Basquiroto de Souza, X. Yao, E. Benhelal, A. Akbari, W. Duan, Graphene-based nanosheets for stronger and more durable concrete: a review, Constr. Build. Mater. 183 (2018) 642–660, https://doi.org/10.1016/j.conbuildmat.2018.06.201.
[5] I. Papanikolaou, N. Arena, A. Al-Tabbaa, Graphene nanoplatelet reinforced concrete for self-sensing structures – a lifecycle assessment perspective, J. Clean. Prod. 240 (2019), https://doi.org/10.1016/j.jclepro.2019.118202 118202.
[6] Ozbulut OE, Jiang Z, Harris DK. Exploring scalable fabrication of self-sensing cementitious composites with graphene nanoplatelets. *Smart Materials and Structures* 2018; Vol 27 (11), 115029. DOI: 10.1088/1361-665X/aae623.
[7] A.S.J. Suiker, R.J.M. Wolfs, S.M. Lucas, T.A.M. Salet, Elastic buckling and plastic collapse during 3D concrete printing, Cem. Concr. Res. 135 (2020), https://doi.org/10.1016/j.cemconres.2020.106016 106016.
[8] V.C. Li, F.P. Bos, K. Yu, W. McGee, T.Y. Ng, S.C. Figueiredo, K. Nefs, V. Mechtcherine, V.N. Nerella, J. Pan, G.P.A.G. Van Zijl, J.P. Kruger, On the emergence of 3D printable engineered, strain hardening cementitious composites (ECC/SHCC), Cem. Concr. Res. 132 (2020), https://doi.org/10.1016/j.cemconres.2020.106038 106038.
[9] H. Baoguo, Y. Xun, O. Jinping, Effect of water content on the piezoresistivity of MWNT/cement composites, J. Mater. Sci. 45 (14) (2010) 3714–3719, https://doi.org/10.1007/s10853-010-4414-7.

[10] H. Liu, A. Deshmukh, N. Salowitz, J. Zhao, K. Sobolev, Resistivity signature of graphene-based fiber-reinforced composite subjected to mechanical loading, Front. Mater. 9 (2022), https://doi.org/10.3389/fmats.2022.818176 818176.

[11] S. Wen, D.D.L. Chung, Uniaxial compression in carbon fiber-reinforced cement, sensed by electrical resistivity measurement in longitudinal and transverse directions, Cem. Concr. Res. 31 (8) (2001) 1289–1294, https://doi.org/10.1016/S0008-8846(00)00304-5.